

RESEARCH PAPER

CPW-fed circular-shaped fractal antenna with three iterations for UWB applications

SARTHAK SINGHAL, ANKIT PANDEY AND AMIT KUMAR SINGH

A coplanar waveguide (CPW)-fed circular-shaped fractal antenna with third iterative orthogonal elliptical slot for ultra-wideband applications is presented. The bandwidth is enhanced by using successive iterations of radiating patch, CPW feedline, and tapered ground plane. An impedance bandwidth of 2.9–20.6 GHz is achieved. The designed antenna has omnidirectional radiation patterns along with average peak realized gain of 3.5 dB over the entire frequency range of operation. A good agreement is observed between the simulated and experimental results. This antenna structure has the advantages of miniaturized size and wide bandwidth in comparison to previously reported fractal structures.

Keywords: Antennas and Propagation for Wireless Systems, Wireless Systems and Signal Processing (SDR, MIMO, UWB, etc.)

Received 15 June 2015; Revised 18 September 2015; Accepted 21 September 2015; first published online 12 October 2015

I. INTRODUCTION

In 2002, Federal Communication Commission allocated the frequency spectrum from 3.1 to 10.6 GHz for unlicensed ultra-wideband (UWB) applications. UWB communication systems offer the advantages of higher transmission rate and lower power consumption over conventional wireless communication systems [1]. UWB technology is integrated with the wireless communication systems by using microstrip antenna structures. These antenna structures have gained a lot of attention for commercial and military applications due to their advantages such as low profile, low-cost, easy fabrication, easy integration, etc. The characteristics of narrow bandwidth and low efficiency are limiting their usage in UWB systems. The dimensions of a conventional microstrip antenna are of the order of half-wavelength to radiate efficiently at the desired frequency. As the size of the antenna becomes less than $\lambda/2$, the radiation of the antenna along with other antenna parameters deteriorates. To enhance the impedance bandwidth and miniaturize the antenna size below half-wavelength dimensions, several techniques have been already used. Application of fractal geometry to antenna structures is proven to be a good method among those techniques. The fractal geometry miniaturizes the antenna size and enhances the antenna bandwidth due to its properties of space filling and self-similarity [2]. Several fractal planar antenna structures having miniaturized dimensions and multiband/wideband performance are already reported in the literature [3–8]. They still have the problem of large size or less bandwidth.

In this paper, an orthogonal elliptical slot-loaded circular-shaped fractal antenna is presented. Three iterations of orthogonal elliptical slots are loaded onto the circular radiating patch with tapered coplanar waveguide (CPW) ground plane to enhance the overall bandwidth of the antenna. It has a stable, omnidirectional radiation pattern with an average peak gain of 3.5 dB.

II. ANTENNA DESIGN

The geometry of the designed antenna structure is illustrated in Fig. 1. The optimized dimensions of the antenna structure are listed in Table 1. It is designed on 1.6 mm thick FR-4 substrate having relative permittivity of 4.4 and loss tangent of 0.02. The overall dimensions of substrate are $29 \times 25 \times 1.6 \text{ mm}^3$. It consists of a circular patch loaded with three iterations of orthogonal elliptical slots, stepped feedline, and tapered coplanar waveguide ground plane. The optimization of antenna dimensions is carried out by varying one variable at a time and keeping all other variables at constant values. The design, simulation, and analysis of the antenna structure is done by using finite-element method based Ansoft's High Frequency Structure Simulator (HFSS) version 11 [9].

Initially, a CPW-fed circular patch with a rectangular ground plane is designed as Antenna 1. To improve the antenna performance by smooth transitions between the ground plane and radiating patch, the upper edge of the ground plane is linearly tapered to derive Antenna 2. Thereafter, the straight feedline is replaced by a single-stepped feedline to achieve Antenna 3.

The iterative structures designed during the designing of third iterative structure are presented in Figs 2(a) to 2(d). To derive the zeroth iteration or initiator, the antenna structure Antenna 3 is loaded with a pair of orthogonal elliptical slots at its center. Further iterations are achieved by scaling

Department of Electronics Engineering, Indian Institute of Technology (BHU), Varanasi, India. Phone: +917376157421

Corresponding author:

S. Singhal

Email: ssinghal.rs.ece@iitbhu.ac.in

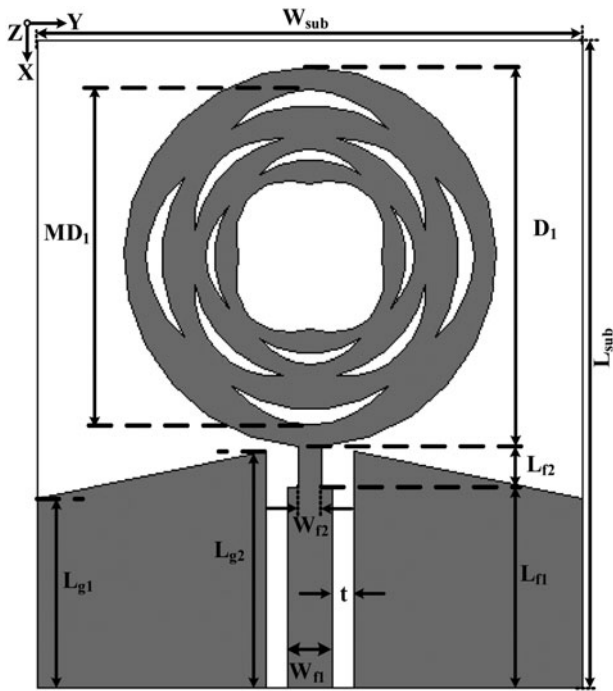


Fig. 1. Geometry of the designed antenna.

Table 1. Optimized dimensions of the parameters.

Parameters	Dimensions	Parameters	Dimensions
L_{sub}	29 mm	L_{g1}	8.6 mm
W_{sub}	25 mm	L_{g2}	10.7 mm
D_1	17 mm	W_{f1}	2 mm
MD_1	15 mm	t	0.4 mm
a_1	0.75	W_{f2}	1 mm
L_{f1}	10.7 mm	Rot	45°

down the 45° rotated initiator structure by iteration factor and then adding it to the previous iterative structure. This process is continued till the third iteration. Further iterations are not designed due to fabrication limitations and insignificant improvement in the antenna performance.

III. PARAMETRIC ANALYSIS

The performance of an antenna structure gets significantly affected with the variation in the values of its dimensions. To study these effects, two antenna dimensions i.e. width of

stepped feedline, W_{f2} ; and gap between the feedline and ground plane, t , are varied. During the parametric analysis, the value of one parameter is varied at a time by keeping all other parameters at fixed values.

The reflection coefficient versus frequency characteristics of the designed antenna for different values of width of stepped feedline are demonstrated in Fig. 3. It is observed that the impedance matching gets improved with decrease in the stepped feedline width, W_{f2} , from 2 to 1 mm. For $W_{f2} = 2$ mm i.e. straight feedline, three operating bands are achieved. In case of $W_{f2} = 1.5$ mm, the impedance matching at frequencies above 12 GHz is slightly improved and the higher band edge frequency is also shifted toward lower frequency. For further reduction in the stepped feedline width i.e. $W_{f2} = 1$ mm, the impedance matching is improved in the whole operating band of 2.9–20.2 GHz.

Reflection coefficient versus frequency characteristics for different values of gap between the feedline and ground plane are shown in Fig. 4. It is observed that the coupling between the feedline and ground plane decreases with increase in the value of t from 0.4 to 0.6 mm. This decrease in the coupling resulted into deterioration of impedance matching which led to reduction of impedance bandwidth.

IV. RESULTS AND DISCUSSION

The comparison of iterative structures in terms of their reflection coefficient characteristic is shown in Fig. 5 and also listed in Table 2. It is observed that with the increase in the number of iterations, the electrical length of the patch increases resulting into shifting of lower band edge toward lower frequency which improves the lower band. Also with the increase in the number of iterations, the path of the current flow increases which improves the impedance matching thereby, reducing the multi-band characteristics into a single wideband characteristics.

The designed antenna structure is again simulated by using finite integration technique (FIT)-based CST Microwave Studio (CST MWS) [4] to verify the results obtained from HFSS. The antenna is fabricated on T-Tech QC-5000 micro-milling machine. The prototype of the designed antenna is shown in Fig. 6. The experimental reflection coefficient is measured on Anritsu Vector Network Analyzer (VNA) Master MS2038C (5–20 GHz). The comparison of simulated and measured reflection coefficient versus frequency characteristics is depicted in Fig. 7 and also listed in Table 3. It is observed that the measured results are in close agreement with the simulated results.

The comparison for the designed antenna structure with the previously reported structures in terms of their size and bandwidth are presented in Table 4. It is observed that the

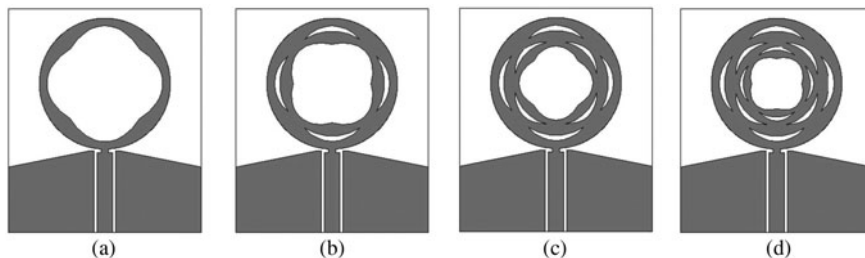


Fig. 2. Four iterations of the antenna structure: (a) zeroth iteration; (b) first iteration; (c) second iteration; and (d) third iteration.

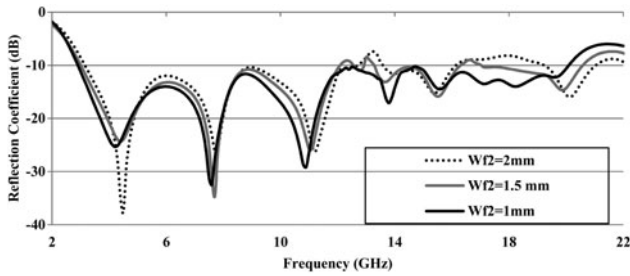


Fig. 3. Variation of reflection coefficient characteristics for different values of $W/2$.

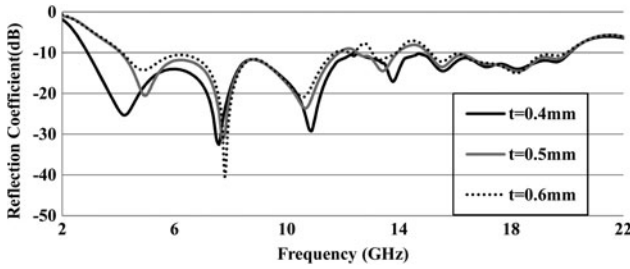


Fig. 4. Variation of reflection coefficient characteristics for different values of t .

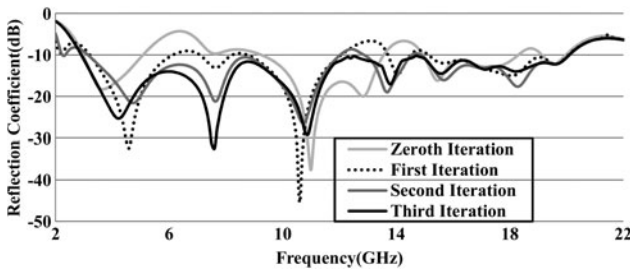


Fig. 5. Reflection coefficient versus frequency characteristics for four iterations of the designed antenna.

Table 2. Comparison of the four iterations of the designed antenna.

Iterations	f_L (GHz)	f_H (GHz)	BW (GHz)	f_L (GHz)	f_H (GHz)	BW (GHz)
Zeroth	3.2	5	1.8	9	13.5	4.5
First	3.1	6	2.9	6.8	12	5.2
Second	3	12	9.5	12.5	20.4	7.9
Third	2.9	20.2	17.3	-	-	-

designed antenna has a size reduction upto 82.43% along with a bandwidth of 17.7 GHz.

The variation of the simulated real and imaginary parts of the input impedance with respect to frequency is shown in Fig. 8. It is observed that the real part of input impedance is varying close to 50 Ω , and imaginary part of impedance is varying near to 0 Ω . Thus, proper impedance matching is achieved between the coaxial cable and the patch antenna within the operational bandwidth.

The simulated current density plot of the designed antenna at different frequencies is shown in Fig. 9. From Figs 9(a) and 9(b), it is observed that at the lower frequencies the maximum

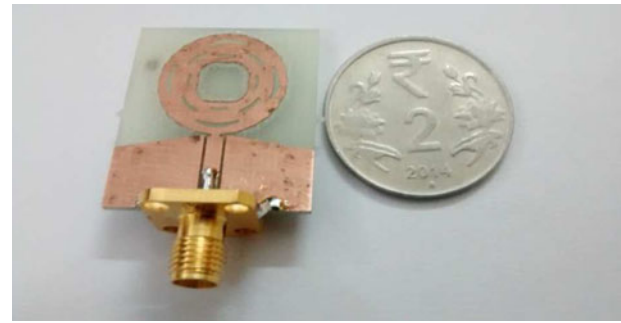


Fig. 6. Prototype of the designed antenna structure.

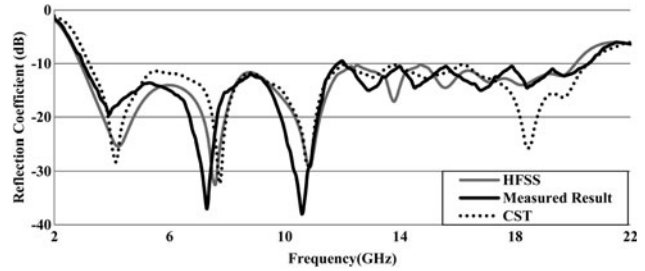


Fig. 7. Comparison of simulated and experimental reflection coefficient characteristics of the designed antenna structure.

Table 3. Comparison of the simulated and measured results of the designed antenna.

Methods	f_L (GHz)	f_H (GHz)	BW (GHz)	BW (%)
HFSS	2.9	20.2	17.3	149.78
CST	3.1	20.6	17.5	147.67
Measured	2.9	20.6	17.7	150.63

Table 4. Comparison of the designed antenna with other antennae in terms of dimensions and bandwidth.

Sl. no.	Antennas	Size (mm ²)	Size reduction (%)	BW (GHz)	BW (%)
1	[3]	30 × 25	3.33	4.4–11	85.71
2	[4]	31 × 32	26.91	5–14	94.73
3	[5]	39.2 × 43.5	57.48	2.28–12	136.13
4	[6]	43 × 51	66.94	2.46–13.46	138.19
5	[7]	50 × 67	78.36	2.05–6.25	101.20
6	[8]	63.5 × 65	82.43	2.55–11.84	129.11
7	[10]	30 × 30	24.14	3.02–13.27	125.84
8	Proposed antenna	29 × 25	-	2.9–20.6	126.08

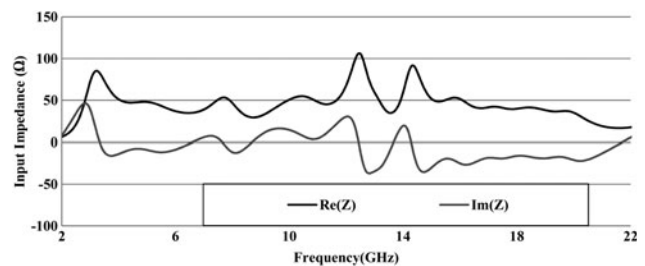


Fig. 8. Variation of real and imaginary parts of input impedance of the designed antenna structure.

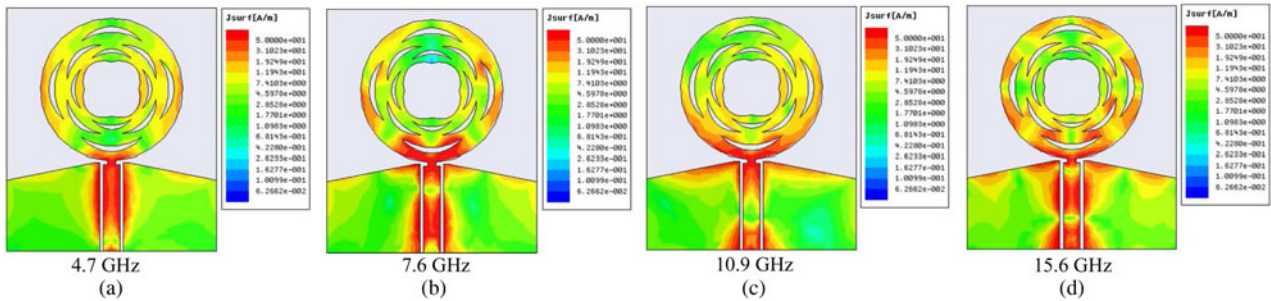


Fig. 9. Surface current density distribution of the designed structure. (a) 4.7 GHz, (b) 7.6 GHz, (c) 10.9 GHz, and (d) 15.6 GHz.

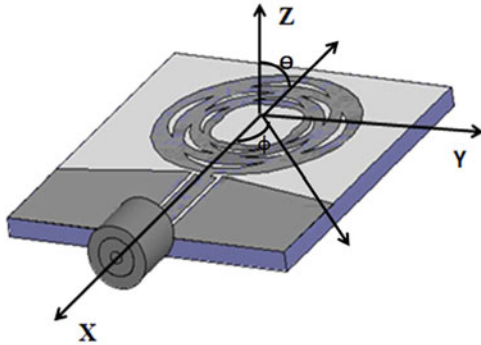


Fig. 10. Radiation pattern measurement setup arrangement for the designed antenna.

current is concentrated mainly on the lower outer edges. As the frequency increases, the current density is shifted more on the upward edges and towards the inner part of the patch as shown in Fig. 10(c). Further as the frequency increases the current density further distributes itself in the whole patch indicating its good response at the higher frequency [11].

The setup for the measurement of radiation pattern is shown in Fig. 10. The antenna is placed along the negative X -axis. The Z -axis is perpendicular to the plane of the antenna. The angle " ϕ " is simulated from X -axis in the anti-clockwise direction and angle " θ " is simulated from the Z -axis in the clockwise direction.

The radiation patterns in both planes at resonant frequencies are shown in Figs 11(a) to 11(d). The patterns clearly indicate that the antenna has an omnidirectional pattern in H -plane and bidirectional in E -plane in the UWB range. As

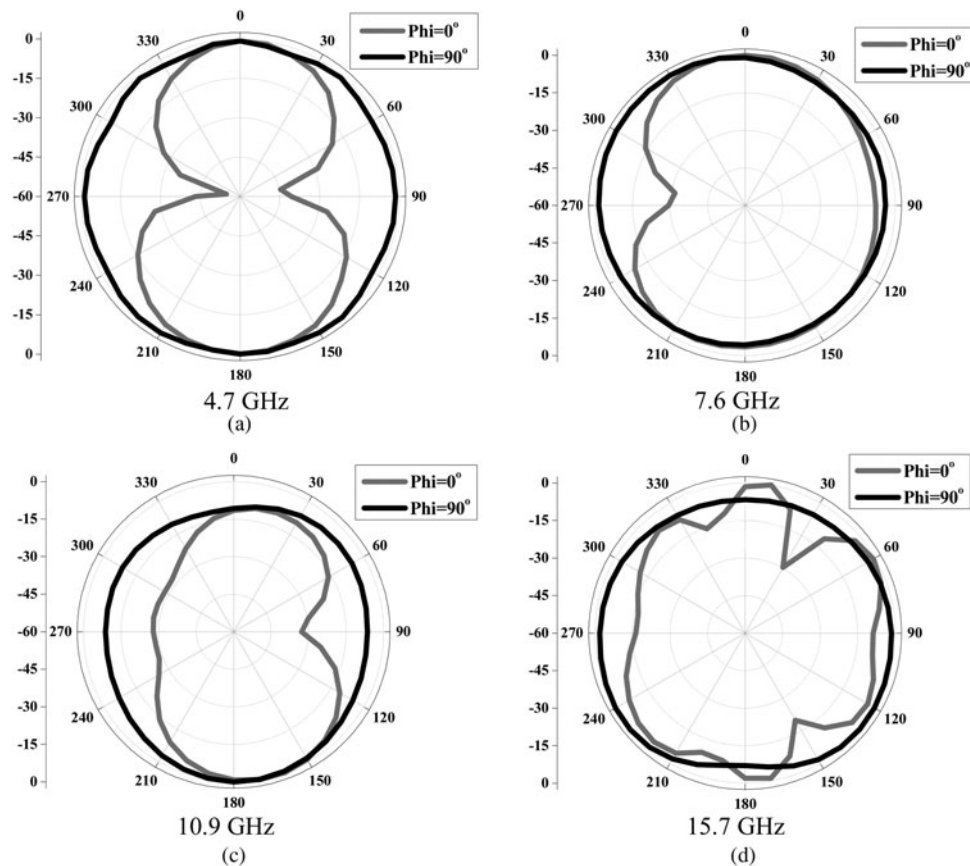


Fig. 11. Radiation patterns of the designed antenna in E - and H -planes at resonance frequencies: (a) 4.7 GHz, (b) 7.6 GHz, (c) 10.9 GHz, and (d) 15.7 GHz.

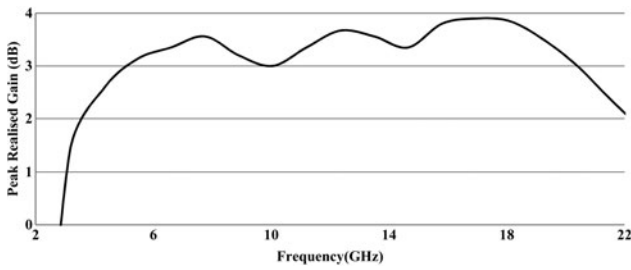


Fig. 12. Variation of peak realized gain with frequency for the designed antenna structure.

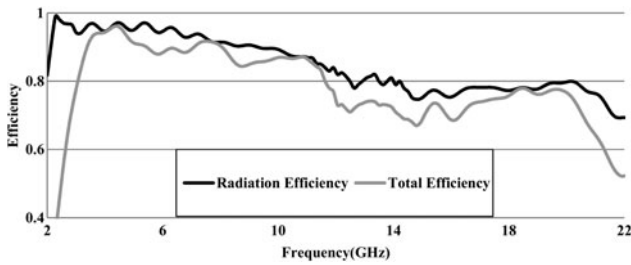


Fig. 13. Simulated variation of radiation and total efficiencies with frequency.

the frequency increases above 10.9 GHz, as shown in Figs 11(c) and 11(d), the radiation pattern started distorting. At higher frequency, the radiation pattern is distorted because of the presence of higher modes.

The variation of the peak gain with respect to frequency is shown in Fig. 12. The peak gain of the antenna remains almost constant throughout the spectrum. The gain of the antenna varies between the maximum of 3.9 dB and minimum of 2 dB with an average gain of 3.6 dB. The gain of the antenna slightly increases with the increase in the frequency due to increase in the effective area of antenna at higher frequency [6].

Fig. 13 shows the variation of radiation and the total efficiency of the antenna with frequency. It is observed that the antenna has more than 75% radiation efficiency throughout the useful band. Also the total efficiency is more than 65%.

V. TIME-DOMAIN ANALYSIS

For the practical implementation of UWB antennas, its time-domain response needs to be analyzed. For this purpose, two identical copies of the same antenna are placed at a distance of 30 cm from each other in two configurations i.e. the face-to-face and side-by-side configurations. Two configurations of designed antenna structure used in time-domain analysis are as shown in Figs 14(a) and 14(b). Time domain analysis is carried out using CST MWS [12]. A Gaussian pulse is transmitted by the antenna and is received at the receiver side. The normalized amplitude of the transmitted and received signals for the face-to-face and side-by-side is shown in Fig. 15. The figure clearly indicates that the received pulse has a very less distortion at the receiver side. The correlation coefficient or the fidelity factor is given by

$$F = \max \left[\frac{\int_{-\infty}^{\infty} s_t(t)s_r(t - \tau)dt}{\int_{-\infty}^{\infty} |s_t(t)|^2 dt \int_{-\infty}^{\infty} |s_r(t)|^2 dt} \right],$$

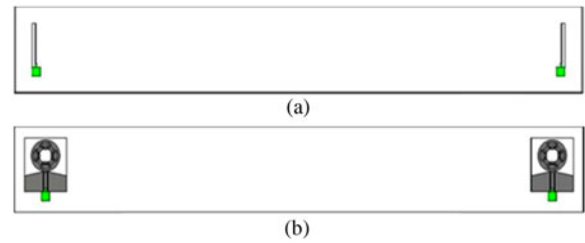


Fig. 14. Time-domain analysis configurations: (a) face-to-face arrangement and (b) side-by-side arrangement.

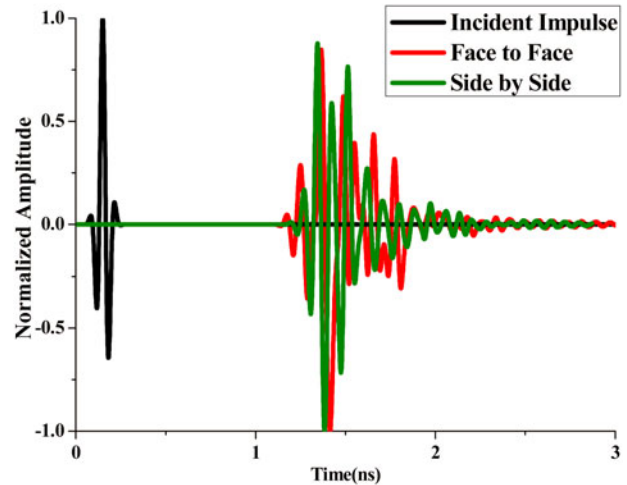


Fig. 15. Simulated normalized amplitudes of the transmitted and received pulses during the time-domain analysis of the circular-shaped fractal antenna.

Table 5. Fidelity factor (in %) for face-to-face and side-by-side configurations.

Configuration	Face-to-face	Side-by-side
Fidelity factor	85.35	80.21

where, $s_t(t)$ and $s_r(t)$ are the transmitted and received signals and “ τ ” is the delay. From Table 5, it is observed that a good fidelity factor is achieved in both configurations. If the fidelity factor is equal to 1, then there is perfect match between the transmitted and the received signals.

The variation in the group delay for the face-to-face and side-by-side configurations, are shown in Fig. 16. It is

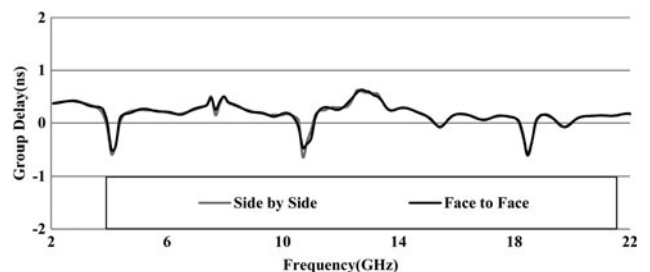


Fig. 16. Variation of group delay with frequency for face-to-face and side-by-side configurations.

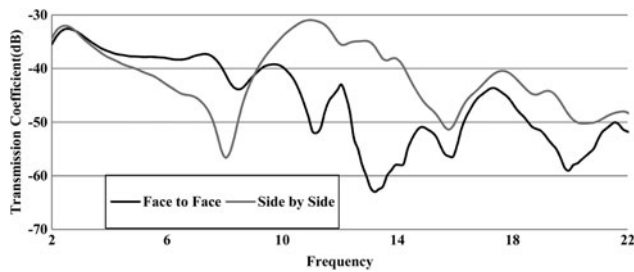


Fig. 17. Variation of transmission coefficient magnitude with frequency for face-to-face and side-by-side configurations.

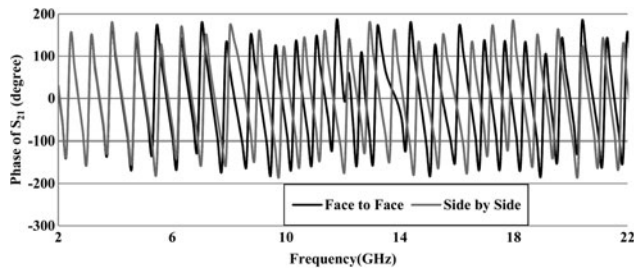


Fig. 18. Variation of phase of S_{21} with frequency for face-to-face and side-by-side configurations.

observed that the group delay is not more than 1 ns in the whole UWB spectrum.

The variation of transmission coefficient S_{21} is shown in Fig. 17. The result clearly suggests that the variation between the minimum and maximum values is less than 30 dB for face-to-face as well as side-by-side configuration. This clearly suggests that variation in the transmission coefficient throughout the spectrum is not large. The variation of the phase of the transmission coefficient for the face-to-face and side-by-side configurations is shown in Fig. 18. The linear phase response for both the configurations indicates that very less distortion will be present in the transmission and reception of the signal.

VI. CONCLUSION

A compact size circular-shaped fractal antenna is fabricated which gives satisfactory response from 2.9 to 20.6 GHz with peak realized gain of around 3.5 dB. The radiation pattern is almost constant throughout the UWB spectrum. The antenna will find suitable application in the field of Passive Sensors in satellite (above 4.95 GHz), Mobile Satellite Communication applications (7.25–7.375 GHz), and Space Research (8.4–8.45 GHz) [13].

ACKNOWLEDGEMENTS

Sarthak Singhal and Ankit Pandey are very grateful to the Ministry of Human Resource Development, Government of India, for providing the financial support in the form of teaching assistantship.

REFERENCES

- [1] Federal Communication Commission: First Order and Report: Revision of Part 15 of the Commission's Rules Regarding UWB Transmission Systems, April 22, 2002.
- [2] Best, S.R.: A comparison of the resonant properties of small space-filling fractal antennas. *IEEE Antennas Wireless Propag. Lett.*, **2** (2003), 197–200.
- [3] Jose, S.M.; Lethakumary, B.: CPW-fed step-shaped microstrip antenna for UWB applications. *Microw. Opt. Technol. Lett.*, **57** (2015), 589–591.
- [4] Kumar, R.; Chaubey, P.N.: On the design of tree type ultra wideband fractal antenna for DS-CDMA system. *J. Microw. Optoelectron. Electromagn. Appl.*, **11** (2012), 107–121.
- [5] Ding, M.; Jin, R.; Geng, J.; Wu, Q.: Design of a CPW-fed ultra wideband fractal antenna. *Microw. Opt. Technol. Lett.*, **49** (2007), 173–176.
- [6] Kim, D.J.; Choi, J.H.; Kim, Y.S.: CPW-fed ultrawideband flower shaped circular fractal antenna. *Microw. Opt. Technol. Lett.*, **55** (2013), 1792–1796.
- [7] Kumar, R.; Malathi, P.: On the design of CPW-feed diamond shape fractal antenna for UWB applications. *Int. J. Electron.*, **98** (2011), 1157–1168.
- [8] Kumar, R.; Gaikwad, S.: On the design of nano arm fractal antenna for UWB wireless applications. *J. Microw. Optoelectron. Electromagn. Appl.*, **12** (2013), 158–171.
- [9] Ansoft Corporation: HFSS, High frequency structure simulator version11, Finite element package, Ansoft Corporation, Available at: <http://www.ansoft.com>.
- [10] Lu, J.H.; Yeh, C.H.: Planar broadband arc shaped monopole antenna for UWB system. *IEEE Trans. Antennas Propag.*, **60** (2012), 3091–3095.
- [11] Fallahi, H.; Altasbaf, Z.: Study of a class of CPW-fed monopole antenna with fractal elements. *IEEE Antennas Wireless Propag. Lett.*, **12** (2013), 1484–1487.
- [12] CST Inc.: CST Microwave Studio Suite 2011, CST Inc., Wellesley Hills, MA, 2007.
- [13] Electronic Communications Committee (ECC): The European table of Frequency Allocations and Applications: ERC Report 25, May 2014.



Sarthak Singhal was born in Gwalior (M.P.), India in 1987. He received his B.E. in Electronics and Telecommunication Engineering from SGSITS, Indore in 2010. He did his M.Tech. (Microwave Engineering) from IIT (Banaras Hindu University (BHU), Varanasi, India in 2012 and is presently working there as a research scholar. His research areas are microstrip antenna and UWB antennas. He worked as an Assistant Professor at MITS, Gwalior for duration of two and half months. He has nine research papers in journals, four in conference proceedings, and a book titled “Design and Analysis of Shorted Gap Coupled Patch Antenna” from LAP LAMBERT Academic Publishing House.



Ankit Pandey was born in Lucknow, India on August 23, 1989. He received his B.Tech. degree in Electronics and Communication Engineering from K. I. E. T. Ghaziabad in 2011 and M.Tech. degree in Microwave Engineering from IIT (BHU), Varanasi in 2015. The portion of M.Tech. Thesis work was carried out by him under the supervision of Dr.

Amit Kumar Singh. His research interest includes microstrip patch antenna and fractal antenna.



Amit Kumar Singh received his B.Tech. degree in Electronics Engineering from VBS Purvanchal University, Jaunpur (U.P.), India in 2001, the M.E. degree in Communication Systems from Government Engineering College, Jabalpur (M.P.), India in 2003, and his Ph.D. degree from the IIT (BHU), Varanasi in 2010, respectively. From May 2005

to September 2006, he was a Junior Research Fellow and

Senior Research Fellow at the Faculty of Engineering and Technology, BHU, Varanasi, India. From September 2006 to October 2007, he was a Lecturer in the Department of Electronics and Communication Engineering, B.I.T. SINDRI, Dhanbad, India. He joined the Department of Electronics Engineering, Institute of Technology, BHU, as an Assistant Professor in October 2007. He is working as an Assistant Professor in the Electronics Engineering Department in IIT (BHU) since June 2012, till date. His research interest includes the areas of design of millimeter frequency antennas, feeds for parabolic reflectors, dielectric resonator antennas, microstrip antennas, EBG, artificial magnetic conductors, soft and hard surfaces, phased array antennas, and computer-aided design for antennas. He has published over 38 journal articles and conference articles.